

Large- D Expansion from Variational Perturbation Theory

Sebastian F. Brandt*

Department of Physics, Campus Box 1105, Washington University in St. Louis, MO 63130-4899, USA

Axel Pelster†

Universität Duisburg-Essen, Campus Essen, Fachbereich Physik, Universitätsstraße 5, 45117 Essen, Germany

(Dated: September 9, 2021)

We derive recursively the perturbation series for the ground-state energy of the D -dimensional anharmonic oscillator and resum it using variational perturbation theory (VPT). From the exponentially fast converging approximants, we extract the coefficients of the large- D expansion to higher orders. The calculation effort is much smaller than in the standard field-theoretic approach based on the Hubbard-Stratonovich transformation.

PACS numbers: 02.30.Mv, 03.65.-w, 12.38.Cy

I. INTRODUCTION

The properties of nontrivial physical systems can only be calculated via efficient approximation schemes. Most easily accessible are perturbation expansions, but they are usually divergent and need resummation. To this end, a variational approach was developed by Feynman and Kleinert [1], which has been systematically extended to an efficient nonperturbative approximation scheme called *variational perturbation theory* (VPT) [2, 3, 4, 5]. It allows the conversion of divergent weak-coupling into convergent strong-coupling expansions and has been applied successfully in various fields, such as quantum mechanics, quantum statistics, condensed matter physics, and critical phenomena. In fact, the most accurate critical exponents come from this theory [6], as has been verified by recent satellite experiments [7].

The convergence of VPT has been analyzed up to very high orders for the ground-state energy of the one-dimensional anharmonic oscillator

$$V(x) = \frac{1}{2} \omega^2 x^2 + g x^4 \quad (1)$$

and was found to be exponentially fast [8, 9]. This surprising result has been confirmed later by studying other physical systems and was proven to hold on general grounds [3, 4]. Furthermore, the exponential convergence seems to be uniform with respect to other system parameters. In this manner, the variational resummation of perturbation series yields approximations which are generically reasonable for all temperatures [10, 11, 12], space and time coordinates [13, 14, 15, 16], magnetic field strengths [17], coupling constants [18, 19, 20], etc.

In this paper, we show that the exponential convergence of VPT is uniform with respect to the space dimension D . To this end, we consider the D -dimensional generalization of the anharmonic oscillator (1), i.e.

$$V(\mathbf{x}) = \frac{1}{2} \omega^2 \mathbf{x}^2 + g (\mathbf{x}^2)^2 \quad (2)$$

with $\mathbf{x} = (x_1, \dots, x_D)$, and determine its ground-state energy as a function of the coupling constant g . In Section II, we derive the corresponding weak-coupling series by evaluating connected vacuum diagrams. In Section III, we show how this perturbation series can be obtained more efficiently by means of Bender-Wu-like recursion relations [21]. In Section IV, we resum the weak-coupling series by applying VPT and examine the resulting convergence, which is again exponentially fast and improves uniformly with increasing dimension D . In Section V, we show that the latter observation is not surprising, since the ground-state energy of the anharmonic oscillator (2) can be determined with the help of a systematic large- D expansion. In Section VI, we apply VPT to extract the large- D expansion to higher orders, which have so far been inaccessible to other methods.

*Electronic address: sbrandt@physics.wustl.edu

†Electronic address: pelster@uni-essen.de

II. PERTURBATION THEORY

The perturbation series for the ground-state energy of the anharmonic oscillator (2) can be calculated from connected vacuum diagrams. Up to the second order in the coupling constant g , the ground-state energy is given by the Feynman diagrams

$$E = \frac{\omega}{2} - \lim_{\beta \rightarrow \infty} \frac{1}{\beta} \left\{ \frac{1}{8} \text{ (loop)} + \frac{1}{48} \text{ (double loop)} + \frac{1}{16} \text{ (triple loop)} + \dots \right\}, \quad (3)$$

with the propagator

$$a \bullet \begin{array}{c} i \quad j \\ \hline \text{---} \end{array} b \equiv \frac{\delta_{ij}}{2\omega} e^{-\omega|\tau_a - \tau_b|} \quad (4)$$

and the vertices

$$i \begin{array}{c} j \\ \bullet \\ a \quad k \\ \hline l \end{array} \equiv -\frac{g}{3} \left\{ \delta_{ij} \delta_{kl} + \delta_{ik} \delta_{jl} + \delta_{il} \delta_{jk} \right\} \int_0^\beta d\tau_a. \quad (5)$$

The connected vacuum diagrams (3) are derived most easily by an efficient graphical recursion method [22]. Evaluating these Feynman diagrams produces the following analytic expression for the ground-state energy:

$$E = \frac{D\omega}{2} + \frac{D(D+2)g}{4\omega^2} - \frac{D(2D^2+9D+10)g^2}{8\omega^5} + \dots \quad (6)$$

Only low perturbation orders are accessible by this procedure. If we want to study higher orders, we better use Bender-Wu-like recursion relations [21].

III. BENDER-WU-LIKE RECURSION RELATIONS

The potential (2) of the D -dimensional anharmonic oscillator is rotationally symmetric. Hence, the ground-state wave function depends only on the distance $x = |\mathbf{x}|$. We solve the corresponding Schrödinger eigenvalue equation

$$\left[-\frac{1}{2} \left(\frac{\partial^2}{\partial x^2} + \frac{D-1}{x} \frac{\partial}{\partial x} \right) + \frac{1}{2} \omega^2 x^2 + g x^4 \right] \psi(x) = E \psi(x) \quad (7)$$

as follows. We write the wave function $\psi(x)$ as

$$\psi(x) = \left(\frac{\omega}{\pi} \right)^{1/4} \exp \left[-\frac{1}{2} \hat{x}^2 + \phi(\hat{x}) \right], \quad (8)$$

with the abbreviation $\hat{x} = x\sqrt{\omega}$, and expand the exponent in powers of the dimensionless coupling constant $\hat{g} = g/\omega^3$ by using

$$\phi(\hat{x}) = \sum_{k=1}^{\infty} \phi_k(\hat{x}) \hat{g}^k. \quad (9)$$

The $\phi_k(\hat{x})$ are expanded in powers of the rescaled coordinate \hat{x} :

$$\phi_k(\hat{x}) = \sum_{m=1}^{k+1} c_m^{(k)} \hat{x}^{2m}. \quad (10)$$

For the ground-state energy we make the ansatz

$$E = \omega \left(\frac{D}{2} + \sum_{k=1}^{\infty} \epsilon_k \hat{g}^k \right). \quad (11)$$

k	ϵ_k
1	$D(D+2)/4$
2	$-D(2D^2+9D+10)/8$
3	$D(8D^3+59D^2+146D+120)/16$
4	$-D(168D^4+1773D^3+7144D^2+12960D+8840)/128$
5	$D(1024D^5+14325D^4+82222D^3+241464D^2+360736D+216960)/256$

TABLE I: Expansion coefficients for the ground-state energy of the anharmonic oscillator (2) up to the fifth order.

Inserting (8)–(11) into (7), we obtain to first order

$$c_1^{(1)} = -\frac{D+2}{4}, \quad c_2^{(1)} = -\frac{1}{4}, \quad \epsilon_1 = \frac{D(D+2)}{4}. \quad (12)$$

For $k \geq 2$, we find the following recursion relation for the expansion coefficients in (10)

$$c_m^{(k)} = \frac{(m+1)(D+2m)}{2m} c_{m+1}^{(k)} + \sum_{l=1}^{k-1} \sum_{n=1}^m \frac{n(m+1-n)}{m} c_n^{(l)} c_{m+1-n}^{(k-l)}, \quad (13)$$

with $c_m^{(k)} \equiv 0$ for $m > k+1$. The expansion coefficients of the ground-state energy follow from

$$\epsilon_k = -D c_1^{(k)}. \quad (14)$$

Table I shows the resulting coefficients ϵ_k up to the fifth order. For $D = 1$, they reduce to the well-known one-dimensional results [21].

IV. VARIATIONAL RESUMMATION

Now we consider the strong-coupling limit of the perturbation series (11). Rescaling the coordinate according to $x \rightarrow xg^{-1/6}$, the Schrödinger equation (7) becomes

$$\left[-\frac{1}{2} \left(\frac{\partial^2}{\partial x^2} + \frac{D-1}{x} \frac{\partial}{\partial x} \right) + \frac{1}{2} g^{-2/3} \omega^2 x^2 + x^4 \right] \psi(x) = g^{-1/3} E \psi(x). \quad (15)$$

Expanding the wave function and the energy in powers of the coupling constant yields

$$\psi(x) = \psi_0(\hat{x}) + \psi_1(\hat{x}) \hat{g}^{-2/3} + \psi_2(\hat{x}) \hat{g}^{-4/3} + \dots, \quad (16)$$

$$E = \omega \hat{g}^{1/3} \left(b_0 + b_1 \hat{g}^{-2/3} + b_2 \hat{g}^{-4/5} + \dots \right). \quad (17)$$

By considering (15) in the limit $g \rightarrow \infty$, we find that the leading strong-coupling coefficient b_0 equals the ground-state energy associated with the Hamilton operator

$$H = -\frac{1}{2} \Delta + (\mathbf{x}^2)^2. \quad (18)$$

Precise numerical values for this ground-state energy for different dimensions D are listed in Table II.

The weak-coupling series (11) is of the form

$$E^{(N)}(g, \omega) = \omega \left[\frac{D}{2} + \sum_{k=1}^N \epsilon_k \left(\frac{g}{\omega^3} \right)^k \right]. \quad (19)$$

$b_0(D = 2)$	1.4771497535779972(31)
$b_0(D = 3)$	2.3936440164822970(37)
$b_0(D = 10)$	10.758265165443755(69)

TABLE II: Numerical results for the leading strong-coupling coefficient b_0 for the ground-state energy of (18).

$b_0(D = 2)$	1.477149753577994356(33)
$b_0(D = 3)$	2.3936440164823030895(77)
$b_0(D = 10)$	10.758265165443797408091(18)

TABLE III: High-precision VPT results from the 80th order for the leading strong-coupling coefficient b_0 in the ground-state energy (2).

The alternating signs and fast growing coefficients in Table I suggest that (19) is a divergent Borel series which is resumable by VPT [2, 3, 4, 5]. To this end, an artificial frequency parameter Ω is introduced in the perturbation series most easily by Kleinert's square-root trick

$$\omega \rightarrow \Omega \sqrt{1 + gr}, \quad (20)$$

with

$$r = \frac{\omega^2 - \Omega^2}{g\Omega^2}. \quad (21)$$

One replaces the frequency ω in the weak-coupling series (19) according to (20) and re-expands the resulting expression in powers of g up to the order g^N . Afterwards, the parameter r is replaced according to (21). This procedure has the effect that the power series of order N for the ground-state energy becomes dependent on the variational parameter Ω :

$$E^{(N)}(g, \omega, \Omega) = \sum_{k=0}^N \epsilon_k g^k \Omega^{1-3k} \sum_{l=0}^{N-k} \binom{(1-3k)/2}{l} \left(\frac{\omega^2}{\Omega^2} - 1 \right)^l. \quad (22)$$

The influence of Ω is then optimized according to the principle of minimal sensitivity [23]: the ground-state energy to N th order is approximated by

$$E^{(N)} = E^{(N)}(g, \omega, \Omega^{(N)}), \quad (23)$$

where $\Omega^{(N)}$ denotes that value of the variational parameter for which $E^{(N)}(g, \omega, \Omega)$ has an extremum or a turning point.

As an example, consider the weak-coupling series (19) to first order:

$$E^{(1)} = \frac{D\omega}{2} + \frac{D(D+2)}{4\omega^2} g. \quad (24)$$

Inserting (20), re-expanding in g to first order, and taking into account (21), we find

$$E^{(1)}(g, \omega, \Omega) = \frac{D\Omega}{4} + \frac{D\omega^2}{4\Omega} + \frac{D(D+2)}{4\Omega^2} g. \quad (25)$$

Extremizing this and going to large coupling constants, we obtain the strong-coupling behavior of the variational parameter

$$\Omega^{(1)} = \omega \hat{g}^{1/3} \left(\Omega_0^{(1)} + \Omega_1^{(1)} \hat{g}^{-2/3} + \Omega_2^{(1)} \hat{g}^{-4/3} + \dots \right), \quad (26)$$

with

$$\Omega_0^{(1)} = \sqrt[3]{2(D+2)}, \quad \Omega_1^{(1)} = \frac{\omega^2}{3\sqrt[3]{2(D+2)}}, \quad \Omega_2^{(1)} = \frac{\omega^4}{108(D+2)}, \quad \dots \quad (27)$$

Inserting the result (26), (27) into (25), we obtain the strong-coupling series (17) with the first-order coefficients

$$b_0^{(1)} = \frac{3D}{8} \sqrt[3]{2(D+2)}, \quad b_1^{(1)} = \frac{D\omega^2}{4\sqrt[3]{2(D+2)}}, \quad b_2^{(1)} = -\frac{D\omega^4}{48(D+2)}, \quad \dots \quad (28)$$

For $D = 1$, this reduces to earlier VPT results in Refs. [8, 9].

In order to determine the strong-coupling coefficient b_0 in (17) to higher orders, we proceed as follows. We observe that the strong-coupling behavior of the variational parameter is for any order N of the form

$$\Omega^{(N)} = \omega \hat{g}^{1/3} \left(\Omega_0^{(N)} + \Omega_1^{(N)} \hat{g}^{-2/3} + \Omega_2^{(N)} \hat{g}^{-4/3} + \dots \right) \quad (29)$$

which corresponds to (26). Inserting (29) into (22), the leading strong-coupling coefficient turns out to be given by

$$b_0^{(N)} \left(\Omega_0^{(N)} \right) = \sum_{k=0}^N \sum_{l=0}^{N-k} \binom{(1-3k)/2}{l} (-1)^l \epsilon_k (\Omega_0^{(N)})^{1-3k}, \quad (30)$$

where the inner sum can be further simplified by using [24]

$$\sum_{l=0}^m (-1)^l \binom{\alpha}{l} = (-1)^m \binom{\alpha-1}{m}. \quad (31)$$

Thus, the leading strong-coupling coefficient reduces to

$$b_0^{(N)} (\Omega_0^{(N)}) = \sum_{k=0}^N \binom{(1-3k)/2 - 1}{N-k} (-1)^{N-k} \epsilon_k \left(\Omega_0^{(N)} \right)^{1-3k}. \quad (32)$$

Determining the optimized $\Omega_0^{(N)}$ for which $b_0^{(N)} (\Omega_0^{(N)})$ has an extremum or a turning point then leads to the approximation $b_0^{(N)} (\Omega_0^{(N)})$ of the leading strong-coupling coefficient b_0 .

By carrying the expansion to high orders, VPT yields approximations whose relative deviation from the exact value vanishes exponentially [3, 4]. In our case, we have for large N

$$\frac{|b_0^{(N)}(D) - b_0(D)|}{b_0(D)} \approx \exp \left[A(D) - B(D) N^{1/3} \right], \quad (33)$$

where the exponent $1/3$ is determined by the structure of the strong-coupling series (17). Due to the exponential convergence of VPT, it turns out that the accuracy of our numerical results for the leading strong-coupling coefficients b_0 in Table II is not sufficient for a useful examination of the convergence behavior of VPT in high orders. Therefore, we use our results from the 80th VPT order as a more precise approximation for b_0 . Table III summarizes our high-precision VPT results, where in each case the uncertainty of b_0 has been estimated by examining the deviation from the result of the previous order. For $D = 2$ and $D = 10$, the VPT results lie within the error margins of the numerical results. However, this is not the case for $D = 3$, where the VPT result lies just outside of the corresponding numerical error margins. We attribute this discrepancy to an overly optimistic error estimate for the numerical result. The precision of the results shown in Table III improves with increasing dimension, which already indicates that the calculation converges faster in higher dimensions. Figure 1 shows the convergence of the VPT results for the three different cases. Fitting the data to straight lines yields for the parameters $A(D)$ and $B(D)$ in (33):

$$A(D=2) = 5.98(72), \quad B(D=2) = 9.89(23), \quad (34)$$

$$A(D=3) = 7.43(48), \quad B(D=3) = 10.67(15), \quad (35)$$

$$A(D=10) = 11.89(63), \quad B(D=10) = 13.33(20). \quad (36)$$

Thus, we find that the convergence of the VPT result indeed improves uniformly with increasing dimension D . This tendency does not come as a surprise, since for $D \rightarrow \infty$ the ground-state energy of an oscillator with quartic anharmonicity can be determined exactly as we will see in the subsequent section.

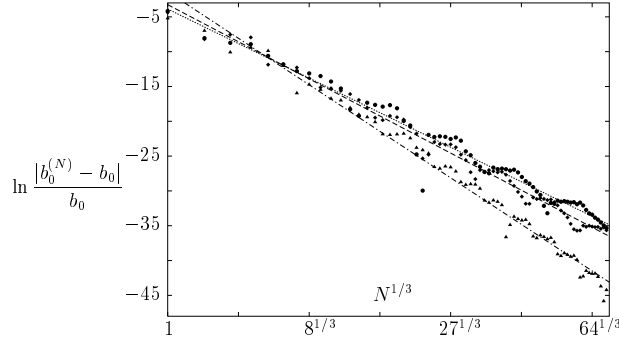


FIG. 1: Logarithm of the relative deviation of the VPT result for the leading strong-coupling coefficient $b_0(D)$ for $D = 2$ (circles), $D = 3$ (diamonds), and $D = 10$ (triangles) plotted as a function of the cubic root of the perturbation order up to 70th order. The dashed lines represent least squares fits of the data to straight lines.

V. LARGE- D EXPANSION

Now, we elaborate the systematic large- D expansion for the ground-state energy of the anharmonic oscillator (2) based on standard field-theoretic methods (see, for instance, Refs. [3, 25, 26]).

A. Effective Potential

We start with the path integral representation of the quantum-statistical partition function at finite temperature T

$$Z = \oint \mathcal{D}\mathbf{x} e^{-\mathcal{A}[\mathbf{x}]}, \quad (37)$$

where the Euclidean action reads

$$\mathcal{A}[\mathbf{x}] = \int_0^\beta d\tau \left\{ \frac{1}{2} \dot{\mathbf{x}}^2(\tau) + \frac{1}{2} \omega^2 \mathbf{x}^2(\tau) + g [\mathbf{x}^2(\tau)]^2 \right\}. \quad (38)$$

The paths are periodic in the imaginary time τ with period $\beta \equiv 1/T$. Applying a Hubbard-Stratonovich transformation,

$$\oint \mathcal{D}\sigma \exp \left\{ - \int_0^\beta d\tau \left[\frac{1}{g} \sigma^2(\tau) + 2i\mathbf{x}^2(\tau)\sigma(\tau) \right] \right\} = \exp \left\{ -g \int_0^\beta d\tau [\mathbf{x}^2(\tau)]^2 \right\}, \quad (39)$$

the $\mathbf{x}(\tau)$ -path integral (37), (38) becomes harmonic and leads to

$$Z = \oint \mathcal{D}\sigma e^{-D\mathcal{A}[\sigma]}, \quad (40)$$

where we have introduced the Euclidean action

$$\mathcal{A}[\sigma] = \frac{1}{Dg} \int_0^\beta d\tau \sigma^2(\tau) + \frac{1}{2} \text{Tr} \ln \left[-\frac{d^2}{d\tau^2} + \omega^2 + 4i\sigma(\tau) \right]. \quad (41)$$

The remaining path integral (40), (41) over $\sigma(\tau)$ is then performed in the limit of large D by regarding the modified coupling constant $\tilde{g} = Dg$ as being independent of D , and by applying the background method [3, 27, 28]. Thus, we take into account order by order the effect of the fluctuations $\delta\sigma(\tau) \equiv \sigma(\tau) - \sigma_0$ of the paths $\sigma(\tau)$ from the background σ_0 . This determines the effective potential

$$V_{\text{eff}}(\sigma_0) = -\frac{1}{\beta} \ln Z \quad (42)$$

in the form of the loop expansion

$$V_{\text{eff}}(\sigma_0) = \sum_{l=0}^{\infty} V_{\text{eff}}^{(l)}(\sigma_0), \quad (43)$$

where the term of loop order l turns out to be of order D^{1-l} .

B. Loop Orders $l = 0$ and $l = 1$

The leading term is the tree-level and follows from evaluating (41) for the background σ_0

$$V_{\text{eff}}^{(0)}(\sigma_0) = D \left[\frac{\sigma_0^2}{\tilde{g}} + \frac{1}{\beta} \ln \left(\sinh \frac{\beta \Omega}{2} \right) \right] \quad (44)$$

with the auxiliary frequency

$$\Omega = \sqrt{\omega^2 + 4i\sigma_0}. \quad (45)$$

The one-loop correction is given by

$$V_{\text{eff}}^{(1)}(\sigma_0) = \frac{1}{2\beta} \text{Tr} \ln G^{-1}(\tau_1, \tau_2), \quad (46)$$

where the operator

$$G^{-1}(\tau_1, \tau_2) = \frac{\delta^2 \mathcal{A}[\sigma]}{\delta \sigma(\tau_1) \delta \sigma(\tau_2)} \Big|_{\sigma(\tau) = \sigma_0} \quad (47)$$

turns out to be

$$G^{-1}(\tau_1, \tau_2) = \frac{2}{\tilde{g}} \delta(\tau_1 - \tau_2) + 8 G_\Omega^2(\tau_1, \tau_2). \quad (48)$$

Here, the correlation function $G_\Omega(\tau_1, \tau_2)$ has the spectral representation

$$G_\Omega(\tau_1, \tau_2) = \sum_{m=-\infty}^{\infty} \frac{e^{-i\omega_m(\tau_1 - \tau_2)}}{\beta(\omega_m^2 + \Omega^2)}, \quad (49)$$

with the Matsubara frequencies $\omega_m = 2\pi m/\beta$. Inserting (49) in (48) yields

$$G^{-1}(\tau_1, \tau_2) = \frac{1}{\beta} \sum_{m=-\infty}^{\infty} G_m^{-1} e^{-i\omega_m(\tau_1 - \tau_2)}, \quad (50)$$

with the coefficients

$$G_m^{-1} = \frac{2}{\tilde{g}} + \frac{8}{\beta} \sum_{m'=-\infty}^{\infty} \frac{1}{(\omega_{m'}^2 + \Omega^2)(\omega_{m-m'}^2 + \Omega^2)}. \quad (51)$$

For the quantum-mechanical ground state energy to be calculated we only need the zero-temperature limit $\beta \rightarrow \infty$ of the above quantum statistical expressions. Thus, we obtain from (44)

$$V_{\text{eff}}^{(0)}(\sigma_0) \rightarrow D \left(\frac{\sigma_0^2}{\tilde{g}} + \frac{\Omega}{2} \right), \quad (52)$$

and the Matsubara sum (51) reduces to an integral,

$$\sum_{m=-\infty}^{\infty} f(\omega_m) \rightarrow \frac{\beta}{2\pi} \int_{-\infty}^{\infty} d\omega_m f(\omega_m), \quad (53)$$

yielding

$$G_m^{-1} = \frac{2}{\tilde{g}} + \frac{8}{\Omega(\omega_m^2 + 4\Omega^2)}. \quad (54)$$

Correspondingly, Eq. (46) becomes

$$V_{\text{eff}}^{(1)}(\sigma_0) = \frac{1}{2\beta} \sum_{m=-\infty}^{\infty} \ln G_m^{-1} \rightarrow \frac{1}{4\pi} \int_{-\infty}^{\infty} d\omega_m \ln G_m^{-1} = \frac{\tilde{\Omega}}{2} - \Omega, \quad (55)$$

where

$$\tilde{\Omega} = 2 \sqrt{\Omega^2 + \frac{\tilde{g}}{\Omega}} \quad (56)$$

denotes another auxiliary frequency.

C. Loop Order $l = 2$

The higher loop orders of the effective potential with $l \geq 2$ consist of all one-particle irreducible vacuum diagrams with the propagator

$$1 \text{ --- } 2 \equiv G(\tau_1, \tau_2) \quad (57)$$

defined by the identity

$$\int_0^\beta d\tau_2 G^{-1}(\tau_1, \tau_2) G(\tau_2, \tau_3) = \frac{1}{D} \delta(\tau_1 - \tau_3) \quad (58)$$

and the vertices

$$\begin{array}{c} 2 \\ | \\ 1 \text{ --- } 3 \\ | \\ n \end{array} \equiv -D \int_0^\beta d\tau_1 \int_0^\beta d\tau_2 \int_0^\beta d\tau_3 \dots \int_0^\beta d\tau_n \frac{\delta^n \mathcal{A}[\sigma]}{\delta \sigma(\tau_1) \delta \sigma(\tau_2) \delta \sigma(\tau_3) \dots \delta \sigma(\tau_n)} \Big|_{\sigma(\tau) = \sigma_0}. \quad (59)$$

For instance, the two-loop contribution is given by the Feynman diagrams

$$V_{\text{eff}}^{(2)}(\sigma_0) = \frac{1}{8} \text{ } \bigcirc \text{ } \bigcirc + \frac{1}{12} \text{ } \bigcirc \text{ } \bigcirc \text{ } \bigcirc \text{ } \bigcirc \quad (60)$$

In order to evaluate (60), we need the third and fourth functional derivatives of the Euclidean action (41). They are given by

$$\frac{\delta^3 \mathcal{A}[\sigma]}{\delta \sigma(\tau_1) \delta \sigma(\tau_2) \delta \sigma(\tau_3)} \Big|_{\sigma(\tau) = \sigma_0} = -64i G_\Omega(\tau_1, \tau_2) G_\Omega(\tau_2, \tau_3) G_\Omega(\tau_3, \tau_1) \quad (61)$$

and

$$\begin{aligned} \frac{\delta^4 \mathcal{A}[\sigma]}{\delta \sigma(\tau_1) \delta \sigma(\tau_2) \delta \sigma(\tau_3) \delta \sigma(\tau_4)} \Big|_{\sigma(\tau) = \sigma_0} &= -256 \left[G_\Omega(\tau_1, \tau_2) G_\Omega(\tau_2, \tau_3) G_\Omega(\tau_3, \tau_4) G_\Omega(\tau_4, \tau_1) \right. \\ &\quad \left. + G_\Omega(\tau_1, \tau_2) G_\Omega(\tau_2, \tau_4) G_\Omega(\tau_4, \tau_3) G_\Omega(\tau_3, \tau_1) + G_\Omega(\tau_1, \tau_3) G_\Omega(\tau_3, \tau_2) G_\Omega(\tau_2, \tau_4) G_\Omega(\tau_4, \tau_1) \right], \end{aligned} \quad (62)$$

where the explicit form of the correlation function $G_\Omega(\tau_1, \tau_2)$ at zero temperature follows from (49) and (53):

$$G_\Omega(\tau_1, \tau_2) = \frac{1}{2\Omega} e^{-\Omega|\tau_1 - \tau_2|}. \quad (63)$$

Furthermore, we have to solve (58) for the propagator (57). Performing at arbitrary temperature the decomposition

$$G(\tau_1, \tau_2) = \frac{1}{\beta} \sum_{m=-\infty}^{\infty} G_m e^{-i\omega_m(\tau_1 - \tau_2)}, \quad (64)$$

the coefficient G_m turns out to be

$$G_m = \frac{1}{D G_m^{-1}}. \quad (65)$$

Using (54) and (65), we evaluate the Matsubara sum (64) at zero temperature according to (53) and obtain

$$G(\tau_1, \tau_2) = \frac{\tilde{g}}{2D} \left[\delta(\tau_1 - \tau_2) - \frac{2\tilde{g}}{\Omega\tilde{\Omega}} e^{-\tilde{\Omega}|\tau_1 - \tau_2|} \right]. \quad (66)$$

From (59) we read off that each vertex is of order D , whereas each propagator is of order $1/D$ due to (66). Thus both Feynman diagrams in (60) are, indeed, of order $1/D$. The first and second Feynman diagram in (60) lead to the expressions

$$\begin{aligned} V_{\text{eff}}^{(2,1)}(\sigma_0) &= \frac{1}{\beta D} \left\{ -\frac{\tilde{g}^2}{2\Omega^4} \left[2I_2(2\Omega) + I_2(4\Omega) \right] + \frac{2\tilde{g}^3}{\Omega^5\tilde{\Omega}} \left[2I_3(\Omega, \Omega, \Omega + \tilde{\Omega}) + I_3(2\Omega, 2\Omega, \tilde{\Omega}) \right] \right. \\ &\quad \left. - \frac{2\tilde{g}^4}{\Omega^6\tilde{\Omega}^2} \left[2I_4(\Omega + \tilde{\Omega}, 0, \Omega, \Omega, 0, \Omega + \tilde{\Omega}) + I_4(\tilde{\Omega}, \Omega, \Omega, \Omega, \Omega, \tilde{\Omega}) \right] \right\}, \end{aligned} \quad (67)$$

$$\begin{aligned} V_{\text{eff}}^{(2,2)}(\sigma_0) &= \frac{1}{\beta D} \left[\frac{2\tilde{g}^3}{3\Omega^6} I_3(2\Omega, 2\Omega, 2\Omega) - \frac{4\tilde{g}^4}{\Omega^7\tilde{\Omega}} I_4(\Omega, \Omega, \tilde{\Omega}, 2\Omega, \Omega, \Omega) + \frac{8\tilde{g}^5}{\Omega^8\tilde{\Omega}^2} I_5(\Omega, \Omega, \tilde{\Omega}, 0, \Omega, 0, \tilde{\Omega}, \Omega, \Omega, \Omega) \right. \\ &\quad \left. - \frac{16\tilde{g}^6}{3\Omega^9\tilde{\Omega}^3} I_6(\Omega, \Omega, \tilde{\Omega}, 0, 0, \Omega, 0, \tilde{\Omega}, 0, 0, 0, \tilde{\Omega}, \Omega, \Omega, \Omega) \right], \end{aligned} \quad (68)$$

respectively. Here we have introduced an abbreviation for multiple integrals with respect to imaginary times:

$$I_n(\Omega_{12}, \dots, \Omega_{1n}, \Omega_{23}, \dots, \Omega_{2n}, \dots) = \int_0^\beta d\tau_1 \int_0^\beta d\tau_2 \dots \int_0^\beta d\tau_n \exp \left(- \sum_{i=1}^n \sum_{j=i+1}^n \Omega_{ij} |\tau_i - \tau_j| \right). \quad (69)$$

Considering the low-temperature limit $\beta \rightarrow \infty$, the first three of these integrals read in closed form [29]:

$$I_2(\Omega_{12}) = \frac{2\beta}{\Omega_{12}}, \quad (70)$$

$$I_3(\Omega_{12}, \Omega_{13}, \Omega_{23}) = \frac{4\beta(\Omega_{12} + \Omega_{13} + \Omega_{23})}{(\Omega_{12} + \Omega_{13})(\Omega_{12} + \Omega_{23})(\Omega_{13} + \Omega_{23})}, \quad (71)$$

$$\begin{aligned} I_4(\Omega_{12}, \Omega_{13}, \Omega_{14}, \Omega_{23}, \Omega_{24}, \Omega_{34}) &= 2\beta \\ &\times \left\{ \frac{1}{\Omega_{12} + \Omega_{13} + \Omega_{24} + \Omega_{34}} \left[\frac{1}{\Omega_{12} + \Omega_{13} + \Omega_{14}} + \frac{1}{\Omega_{14} + \Omega_{24} + \Omega_{34}} \right] \left[\frac{1}{\Omega_{12} + \Omega_{23} + \Omega_{24}} + \frac{1}{\Omega_{13} + \Omega_{23} + \Omega_{34}} \right] \right. \\ &+ \frac{1}{\Omega_{12} + \Omega_{14} + \Omega_{23} + \Omega_{34}} \left[\frac{1}{\Omega_{12} + \Omega_{23} + \Omega_{24}} + \frac{1}{\Omega_{14} + \Omega_{24} + \Omega_{34}} \right] \left[\frac{1}{\Omega_{12} + \Omega_{13} + \Omega_{14}} + \frac{1}{\Omega_{13} + \Omega_{23} + \Omega_{34}} \right] \\ &\left. + \frac{1}{\Omega_{13} + \Omega_{14} + \Omega_{23} + \Omega_{24}} \left[\frac{1}{\Omega_{13} + \Omega_{23} + \Omega_{34}} + \frac{1}{\Omega_{14} + \Omega_{24} + \Omega_{34}} \right] \left[\frac{1}{\Omega_{12} + \Omega_{13} + \Omega_{14}} + \frac{1}{\Omega_{12} + \Omega_{23} + \Omega_{24}} \right] \right\}. \end{aligned} \quad (72)$$

Furthermore, in order to evaluate (68), we need one particular integral with respect to five and six imaginary times, respectively:

$$I_5(\Omega, \Omega, \tilde{\Omega}, 0, \Omega, 0, \tilde{\Omega}, \Omega, \Omega, \Omega) = \frac{\beta(3\tilde{\Omega}^5 + 42\tilde{\Omega}^4\Omega + 227\tilde{\Omega}^3\Omega^2 + 568\tilde{\Omega}^2\Omega^3 + 656\tilde{\Omega}\Omega^4 + 288\Omega^5)}{2\Omega^2(\tilde{\Omega} + \Omega)^2(\tilde{\Omega} + 2\Omega)^4(\tilde{\Omega} + 4\Omega)}, \quad (73)$$

$$I_6(\Omega, \Omega, \tilde{\Omega}, 0, 0, \Omega, 0, \tilde{\Omega}, 0, 0, 0, \tilde{\Omega}, \Omega, \Omega, \Omega) = \frac{3\beta(\tilde{\Omega}^5 + 14\tilde{\Omega}^4\Omega + 73\tilde{\Omega}^3\Omega^2 + 160\tilde{\Omega}^2\Omega^3 + 136\tilde{\Omega}\Omega^4 + 32\Omega^5)}{\tilde{\Omega}\Omega^2(\tilde{\Omega} + \Omega)^2(\tilde{\Omega} + 2\Omega)^4(\tilde{\Omega} + 4\Omega)}. \quad (74)$$

From (44) and (67)–(74) we read off the effective potential for zero temperature up to the order $1/D$:

$$\begin{aligned} V_{\text{eff}}(\sigma_0) &= D \left(\frac{\sigma_0^2}{\tilde{g}} + \frac{\Omega}{2} \right) + \frac{\tilde{\Omega}}{2} - \Omega + \frac{1}{D} \left[-\frac{5\tilde{g}^2}{4\Omega^5} + \frac{\tilde{g}^3(\tilde{\Omega}^3 + 4\tilde{\Omega}^2\Omega + 44\tilde{\Omega}\Omega^2 + 128\Omega^3)}{4\Omega^8\tilde{\Omega}(\tilde{\Omega} + 2\Omega)^2} \right. \\ &- \frac{\tilde{g}^4(3\tilde{\Omega}^5 + 31\tilde{\Omega}^4\Omega + 150\tilde{\Omega}^3\Omega^2 + 392\tilde{\Omega}^2\Omega^3 + 656\tilde{\Omega}\Omega^4 + 480\Omega^5)}{\Omega^9\tilde{\Omega}^2(\tilde{\Omega} + \Omega)(\tilde{\Omega} + 2\Omega)^3(\tilde{\Omega} + 4\Omega)} \\ &+ \frac{4\tilde{g}^5(3\tilde{\Omega}^5 + 42\tilde{\Omega}^4\Omega + 227\tilde{\Omega}^3\Omega^2 + 568\tilde{\Omega}^2\Omega^3 + 656\tilde{\Omega}\Omega^4 + 288\Omega^5)}{\Omega^{10}\tilde{\Omega}^2(\tilde{\Omega} + \Omega)^2(\tilde{\Omega} + 2\Omega)^4(\tilde{\Omega} + 4\Omega)} \\ &\left. - \frac{16\tilde{g}^6(\tilde{\Omega}^5 + 14\tilde{\Omega}^4\Omega + 73\tilde{\Omega}^3\Omega^2 + 160\tilde{\Omega}^2\Omega^3 + 136\tilde{\Omega}\Omega^4 + 32\Omega^5)}{\Omega^{11}\tilde{\Omega}^4(\tilde{\Omega} + \Omega)^2(\tilde{\Omega} + 2\Omega)^4(\tilde{\Omega} + 4\Omega)} \right] + \mathcal{O}\left(\frac{1}{D^2}\right). \end{aligned} \quad (75)$$

The ground-state energy of the anharmonic oscillator (2) is found by extremizing the effective potential (75) with respect to the background σ_0 while taking into account the auxiliary frequencies (45) and (56).

D. Weak-Coupling

In order to cross-check our large- D result, we specialize now to the weak-coupling regime where the extremal background is expanded according to

$$\sigma_0 = -i(s_1\tilde{g} + s_2\tilde{g}^2 + s_3\tilde{g}^3 + s_4\tilde{g}^4 + s_5\tilde{g}^5 + \dots). \quad (76)$$

Inserting (76) into the vanishing first derivative of (75) and re-expanding in \tilde{g} , we obtain a system of equations which are solved by

$$s_1 = \frac{1}{2\omega}, \quad (77)$$

$$s_2 = -\frac{1}{2\omega^4} - \frac{1}{\omega^4 D}, \quad (78)$$

$$s_3 = \frac{5}{4\omega^7} + \frac{45}{8\omega^7 D} + \frac{25}{4\omega^7 D^2}, \quad (79)$$

$$s_4 = -\frac{4}{\omega^{10}} - \frac{59}{2\omega^{10} D} - \frac{73}{\omega^{10} D^2}, \quad (80)$$

$$s_5 = \frac{231}{16\omega^{13}} + \frac{19503}{128\omega^{13} D} + \frac{9823}{16\omega^{13} D^2} + \frac{275}{2\omega^{13} D^3}, \quad \dots \quad (81)$$

Inserting (76)–(81) into (75) and re-expanding in $\tilde{g} = Dg$ yields again the weak-coupling series (11), where the weak-coupling coefficients ϵ_k of Table I are reproduced in the first three terms of order D^{k+1} , D^k , and D^{k-1} .

E. Strong-Coupling

We now derive the large- D expansion for the ground-state energy in the strong-coupling regime. There, we use for the extremal background the ansatz

$$\sigma_0 = -i\tilde{g}^{2/3} \left(S_1 + S_2 \tilde{g}^{-2/3} + \dots \right) \quad (82)$$

and find for the leading coefficient the expansion

$$S_1 = \frac{1}{2^{4/3}} + \left(2^{1/6} \cdot 3^{1/2} - 2^{5/3} \right) \frac{1}{6D} + \left(27 \cdot 6^{1/2} - \frac{73}{2} \right)^{1/3} \frac{1}{18D^2} + \mathcal{O}\left(\frac{1}{D^3}\right). \quad (83)$$

From (75), (82), and (83) we then obtain the strong-coupling series (17) where the leading strong-coupling coefficient has the large- D expansion

$$b_0 = \sum_{k=0}^{\infty} B_k D^{4/3-k}, \quad (84)$$

with

$$B_0 = \frac{3 \cdot 2^{1/3}}{8}, \quad (85)$$

$$B_1 = \frac{3^{1/2} - 2^{1/2}}{2^{1/6}} \approx 0.2831607943221791188446646047948820365123, \quad (86)$$

$$B_2 = -\frac{239}{18 \cdot 2^{2/3} (25 + 12 \cdot 6^{1/2})} \approx -0.1537760559399284913195761085499705701590. \quad (87)$$

Figure 2 shows the leading strong-coupling coefficient (84)–(86) up to the first two orders plotted as a function of the dimension D .

VI. LARGE- D EXPANSION FROM VPT

In this section, we study how the large- D expansion (84) follows from VPT. Thereby, we numerically determine the large- D expansion coefficients up to B_6 with high precision.

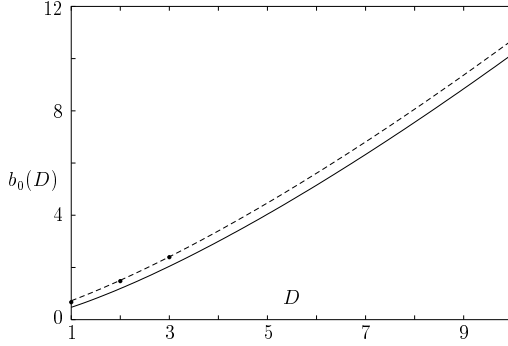


FIG. 2: Strong-coupling coefficient $b_0(D)$ versus dimension D . Solid and dashed lines represent leading and subleading results of the large- D expansion (84)–(86), respectively. For $D = 1$, the dot represents the earlier result from Refs. [8, 9]; for $D = 2, 3, 10$, the dots indicate the highly accurate VPT values obtained from the 80th order, as given in Table III.

A. Coefficients B_1 and B_2

To first order, VPT gives (28), and we obtain the expansion (84) simply by expanding the cubic root in (28) in powers of $1/D$. The first three coefficients in the expansion (84) read

$$B_0^{(1)} = \frac{3 \cdot 2^{1/3}}{8}, \quad B_1^{(1)} = \frac{2^{1/3}}{4}, \quad B_2^{(1)} = -\frac{2^{1/3}}{6}. \quad (88)$$

The leading coefficient (85) is reproduced exactly, while the next two subleading coefficients B_1 and B_2 are missed by 11.2 % and 36.6 %, respectively. In the second order of VPT, Eq. (32) yields

$$b_0^{(2)}(\Omega_0^{(2)}) = \frac{3D\Omega_0^{(2)}}{16} + \frac{D(2+D)}{2(\Omega_0^{(2)})^2} - \frac{D(10+9D+2D^2)}{8(\Omega_0^{(2)})^5}, \quad (89)$$

which has to be extremized with respect to the variational parameter $\Omega_0^{(2)}$. Setting the derivative of (89) to zero, the large- D expansion

$$\Omega_0^{(2)} = D^{1/3} \left(C_0^{(0,2)} + \frac{C_1^{(0,2)}}{D} + \frac{C_2^{(0,2)}}{D^2} + \dots \right) \quad (90)$$

leads to a system of equations for the expansion coefficients whose solutions read

$$C_0^{(2)} = 2^{1/3}, \quad C_1^{(2)} = \frac{13 \cdot 2^{1/3}}{12}, \quad C_2^{(2)} = -\frac{113 \cdot 2^{1/3}}{288}, \quad \dots. \quad (91)$$

Thus, by inserting the optimized variational parameter (90), (91) into (89) and expanding in $1/D$ we obtain the first three coefficients in (84) to second order of VPT:

$$B_0^{(2)} = \frac{3 \cdot 2^{1/3}}{8}, \quad B_1^{(2)} = \frac{7 \cdot 2^{1/3}}{32}, \quad B_2^{(2)} = -\frac{71 \cdot 2^{1/3}}{768}. \quad (92)$$

The leading large- D coefficient B_0 remains the same, whereas the error of the subleading coefficient $B_1^{(2)}$ is reduced to 2.67 % and the next subleading coefficient $B_2^{(2)}$ now comes out with an error of 24.2 %. Figure 3 shows that the VPT approximants $B_1^{(N)}$ and $B_2^{(N)}$ converge exponentially fast to their exact values B_1 and B_2 in (86) and (87). If we had not known the exact analytic result for the subleading coefficients B_1 and B_2 , we could have extracted its value from the VPT approximants as follows. Figure 3 shows that the VPT approximants for odd and even orders converge towards the exact value independently. Extrapolating the values of $B_1^{(\text{odd})}$ and $B_1^{(\text{even})}$ for $N \rightarrow \infty$ leads to the limiting values

$$B_1^{(\text{odd})} \approx 0.28316079432217911884466460479488203808, \quad (93)$$

$$B_1^{(\text{even})} \approx 0.28316079432217911884466460479488203575. \quad (94)$$

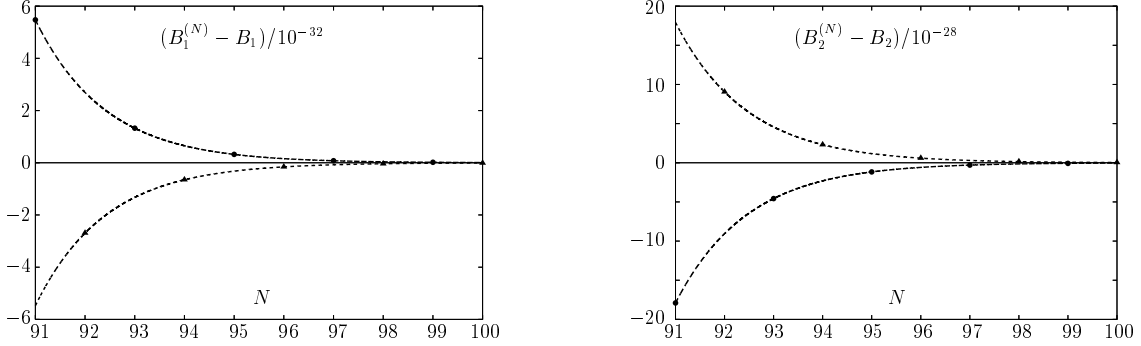


FIG. 3: Deviation of the VPT approximants for $B_1^{(N)}$ and $B_2^{(N)}$ from their exact values B_1 and B_2 in Eqs. (86), (87), respectively. Odd orders are represented by circles; even orders by triangles. The dashed lines represent fits of the data to exponential functions.

Assuming that the exact value lies within this interval, we obtain from this extrapolation method the result

$$B_1^{(\text{extrap})} = 0.2831607943221791188446646047948820369(24). \quad (95)$$

An analogous procedure can be applied to extract a numerical value for the subsequent coefficient B_2 . Applying the extrapolation method for odd and even orders, we obtain the result

$$B_2^{(\text{extrap})} = -0.153776055939928491319576108549961(60). \quad (96)$$

B. Coefficients up to B_6

Figure 4 shows that the VPT approximants for B_1 and B_2 rapidly converge towards their exact values. For the large- D expansion coefficients of higher orders in $1/D$, however, the VPT approximants first fluctuate and then enter the regime of exponentially fast convergence. If we want to obtain the coefficients of the expansion (84) to higher orders and with good accuracy, we must therefore drive our VPT calculation to high orders. To this end, we specialize the expression for the leading strong-coupling coefficient as given in (32) in such a way that we can read off the corresponding large- D expansion. The weak-coupling coefficients for the ground-state energy ϵ_k can be expanded in powers of the spatial dimension D ,

$$\epsilon_k = \sum_{j=1}^{k+1} \epsilon_j^{(k)} D^j, \quad (97)$$

whereas the variational parameter $\Omega_0^{(N)}$ can be expanded in $1/D$:

$$\Omega_0^{(N)} = D^{1/3} \sum_{j=0}^M C_j^{(0,N)} D^{-j}. \quad (98)$$

Here, M denotes the highest order to which we seek to drive the large- D expansion (84). Furthermore, recall the multinomial expansion

$$(x_1 + x_2 + \dots + x_m)^n = \sum_{a_1=0}^n \sum_{a_2=0}^n \dots \sum_{a_m=0}^n \delta \left(n, \sum_{k=1}^m a_k \right) \frac{n!}{a_1! a_2! \dots a_m!} \prod_{l=1}^m x_l^{a_l}, \quad (99)$$

where n is an integer and where the Kronecker delta δ_{ij} is written as $\delta(i, j)$. This multinomial expansion can be generalized to hold for real exponents and infinite series as follows:

$$\begin{aligned} (1 + x_1 + x_2 + \dots)^\alpha &= \sum_{m=0}^{\infty} \left[\sum_{a_1=0}^{\infty} \sum_{a_2=0}^{\infty} \dots \sum_{a_m=0}^{\infty} \delta \left(m, \sum_{l=1}^m l a_l \right) \right. \\ &\quad \times \left. \frac{\Gamma(\alpha + 1)}{\Gamma(\alpha - a_1 - a_2 - \dots - a_m + 1) a_1! a_2! \dots a_m!} \prod_{l=1}^m x_l^{a_l} \right]. \end{aligned} \quad (100)$$

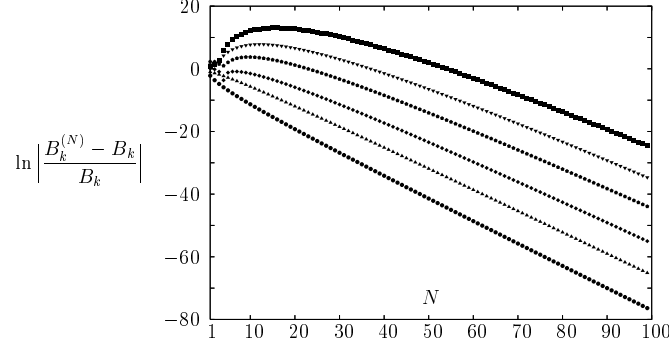


FIG. 4: Logarithm of the relative deviation of the VPT results $B_k^{(N)}$ for the coefficients B_1 through B_6 in the large- D expansion (84) versus the order N of VPT. The lowest curve (circles) is for $B_1^{(N)}$; the uppermost curve (squares) is for $B_6^{(N)}$; intermediate curves are for $B_2^{(N)}$ through $B_5^{(N)}$ ($B_2^{(N)}$: triangles, $B_3^{(N)}$: diamonds, $B_4^{(N)}$: pentagons, $B_5^{(N)}$: upside-down triangles). For $B_1^{(N)}$ and $B_2^{(N)}$ the exact values from (86) and (87) were used in order to determine the relative deviation. For $B_3^{(N)}$ through $B_6^{(N)}$ we used our extrapolation results from Table IV.

Using (97) and (98) in (32) and applying the multinomial expansion (100), we obtain

$$b_0^{(N)}(\Omega_0^{(N)}) = D^{1/3} \left\{ \frac{D}{2} \sum_{j=0}^M C_j^{(0,N)} D^{-j} + \sum_{k=1}^N \binom{(1-3k)/2-1}{N-k} (-1)^{N-k} D^{-k} \left(C_0^{(0,N)} \right)^{1-3k} \right. \\ \left. \times \left[\sum_{j=1}^{k+1} \epsilon_j^{(k)} D^j + \sum_{j=2}^{M+k} \sum_{m=1}^{\min\{j-1, \lfloor (M+j-k)/2 \rfloor - 1\}} \epsilon_{j-m}^{(k)} K_{m,k}^{(N)} D^{j-2m} \right] \right\}, \quad (101)$$

where the coefficients $K_{m,k}^{(N)}$ are given by

$$K_{m,k}^{(N)} = \sum_{a_1=0}^M \sum_{a_2=0}^M \dots \sum_{a_m=0}^M \delta \left(m, \sum_{l=1}^m l a_l \right) \frac{(3k-2+a_1+a_2+\dots+a_m)!}{(3k-2)! a_1! a_2! \dots a_m!} (-1)^{a_1+a_2+\dots+a_m} \prod_{l=1}^m \left(\frac{C_l^{(0,N)}}{C_0^{(0,N)}} \right)^{a_l}. \quad (102)$$

The summation boundaries in (101) are determined by the two conditions that i) $\epsilon_j^{(k)} = 0$ for $j < 1 \vee j > k+1$ and ii) we can neglect contributions containing coefficients $C_k^{(0,N)}$ with $k > M$. Note that a similar expansion holds for the derivative of the leading strong-coupling coefficient with respect to the variational parameter $db_0^{(N)}/d\Omega_0^{(N)}$. Using (101), (102) we can efficiently calculate the VPT approximants to high orders. In each order of VPT, the leading large- D coefficient B_0 comes out exactly. Furthermore, the expansion coefficients $C_k^{(0,N)}$ for the variational parameter are found by solving linear equations. Figure 4 shows the convergence behavior of our VPT approximants for B_1 through B_6 up to $N = 100$. By extrapolating the VPT results $B_k^{(N)}$ for $k \geq 3$ in the limit $N \rightarrow \infty$, we are able to determine the coefficients in the large- D expansion to high accuracy. The numerical results are shown in Table IV.

VII. SUMMARY

We have determined the weak-coupling series of the ground-state energy for the D -dimensional anharmonic oscillator (2) and used variational perturbation theory to extract the coefficients of the large- D expansion to higher orders than accessible by standard field-theoretic methods based on the Hubbard-Stratonovich transformation.

Acknowledgement

We cordially thank Hagen Kleinert for having inspired the present work and for carefully reading the manuscript.

B_3	0.1098507701648367991179224418(38)
B_4	-0.02886373198599697649759(11)
B_5	-0.1695976321261828993(92)
B_6	0.51902738902696(86)

TABLE IV: VPT results for the coefficients in the large- D expansion (84) of the leading strong-coupling coefficient b_0 .

[1] R.P. Feynman and H. Kleinert: Phys. Rev. A **34**, 5080 (1986).
[2] H. Kleinert: Phys. Lett. A **173**, 332 (1993).
[3] H. Kleinert: *Path Integrals in Quantum Mechanics, Statistics, Polymer Physics, and Financial Markets*, Third Edition (World Scientific, Singapore, 2004).
[4] H. Kleinert and V. Schulte-Frohlinde: *Critical Properties of Φ^4 -Theories* (World Scientific, Singapore, 2001).
[5] W. Janke, A. Pelster, H.-J. Schmidt, and M. Bachmann (Editors): *Fluctuating Paths and Fields – Dedicated to Hagen Kleinert on the Occasion of his 60th Birthday* (World Scientific, Singapore, 2001).
[6] H. Kleinert, Phys. Rev. D **60**, 085001 (1999).
[7] J.A. Lipa, J.A. Nissen, D.A. Stricker, D.R. Swanson, and T.C.P. Chui, Phys. Rev. B **68**, 174518 (2003).
[8] W. Janke and H. Kleinert: Phys. Rev. Lett. **75**, 2787 (1995).
[9] H. Kleinert and W. Janke: Phys. Lett. A **206**, 283 (1995).
[10] H. Kleinert and H. Meyer: Phys. Lett. A **184**, 319 (1994).
[11] H. Kleinert, W. Kürzinger, and A. Pelster: J. Phys. A **31**, 8307 (1998).
[12] F. Weißbach, A. Pelster, and B. Hamprecht: Phys. Rev. E **66**, 036129 (2002).
[13] H. Kleinert, M. Bachmann, and A. Pelster: Phys. Rev. A **60**, 3429 (1999).
[14] H. Kleinert, A. Pelster, and M. Putz: Phys. Rev. E **65**, 066128 (2002).
[15] A. Pelster, H. Kleinert, and M. Schanz: Phys. Rev. E **67**, 016604 (2003).
[16] J. Dreger, A. Pelster, and B. Hamprecht: Eur. Phys. J. B (in press).
[17] M. Bachmann, H. Kleinert, and A. Pelster: Phys. Rev. A **62**, 52509 (2000); Phys. Lett. A **279**, 23 (2001).
[18] C.M. Bender, A. Pelster, and F. Weißbach: J. Math. Phys. **43**, 4202 (2002).
[19] A. Pelster, H. Kleinert, and M. Schanz: Phys. Rev. E **67**, 016604 (2003).
[20] S.F. Brandt, H. Kleinert, and A. Pelster: J. Math. Phys. **46**, 032101 (2005).
[21] C.M. Bender and T.T. Wu: Phys. Rev. **184**, 1231 (1969); Phys. Rev. D **7**, 1620 (1973).
[22] H. Kleinert, A. Pelster, B. Kastening, and M. Bachmann: Phys. Rev. E **62**, 1537 (2000).
[23] P.M. Stevenson: Phys. Rev. D **23**, 2916 (1981).
[24] I.S. Gradshteyn and I.M. Ryzhik, *Table of Integrals, Series, and Products* (Academic Press, New York, 1965).
[25] E. Brezin and S.R. Wadia (Editors): *The Large N Expansion in Quantum Field Theory and Statistical Physics: From Spin Systems to 2-Dimensional Gravity*, (World Scientific, Singapore, 1993).
[26] J. Zinn-Justin: *Quantum Field Theory and Critical Phenomena*, 3rd Edition (Oxford Science Publication, New York, 1996).
[27] B. De Witt: *Dynamical Theory of Groups and Fields* (Gordon and Breach, New York, 1965).
[28] R. Jackiw: Phys. Rev. D **9**, 1686 (1974).
[29] More details can be found in: S.F. Brandt: *Beyond Effective Potential via Variational Perturbation Theory* (Diplom thesis, Freie Universität Berlin, 2004): <http://hbar.wustl.edu/~sbrandt/diplomarbeit.pdf>.